Journal of Molecular Modeling (2022) 28:380
https://doi.org/10.1007/s00894-022-05356-9

ORIGINAL PAPER

# Modeling studies on the role of vitamins B1 (thiamin), B3 (nicotinamide), B6 (pyridoxamine), and caffeine as potential leads for the drug design against COVID-19

**Mohammad Aghamohammadi[1] · Mehdi Sirouspour[2] · Arlan S. Goncalves[3,4] · Tanos Celmar Costa França[5,6,7] · Steven R. LaPlante[5] · Parvin Shahdousti[1]**

Received: 28 February 2022 / Accepted: 17 October 2022 / Published online: 7 November 2022


## Abstract

In response to the COVID-19 pandemic, and the lack of effective and safe antivirals against it, we adopted a new approach in which food supplements with vital antiviral characteristics, low toxicity, and fast excretion have been targeted. The structures and chemical properties of the food supplements were compared to the promising antivirals against SARS-COV-2. Our goal was to exploit the food supplements to mimic the topical antivirals' functions but circumventing their severe side effects, which has limited the necessary dosage needed to exhibit the desired antiviral activity. On this line, after a comparative structural analysis of the chemicals mentioned above, and investigation of their potential mechanisms of action, we selected caffeine and some compounds of the vitamin B family and further applied molecular modeling techniques to evaluate their interactions with the RDB domain of the Spike protein of SARS-CoV-2 (*SC2*Spike) and its corresponding binding site on human ACE-2 (*Hss*ACE2). Our results pointed to vitamins B1 and B6 in the neutral form as potential binders to the *Hss*ACE2 RDB binding pocket that might be able to impair the SARS-CoV-2 mechanism of cell invasion, qualifying as potential leads for experimental investigation against COVID-19.

**Keywords** COVID-19 · Caffeine · Vitamin B · Docking · Molecular dynamic simulations

## Introduction

COVID-19, caused by SARS-CoV-2, has brought up transient records of contagiousness rate and fatality so far, and there is not yet a clear overview on how the humanity will take over this pandemic. The main goal of the non-stop ongoing research has been to address the two main prerequisites to control the situation: (1) scientists have attempted to contain the disease spreading by presenting safe vaccines which have been challenged by the high rate of SARS-COV-2 mutation [1], while (2) there have been many attempts to find effective antiviral agents that could cure or at least mitigate the COVID-19 symptoms [2]. On this second line, crystal structures and computational studies on the most conserved proteins in the coronavirus family such as main protease ($M^{pro}$), chymotrypsin-like protease ($3CL^{pro}$) [3], and RNA-dependent RNA polymerase (RdRp) [4] have been exploited for proposing potentially effective antiviral agents. Considering the long way that a new drug has to go to be approved, and the high risk of potential side effects of a new generation of antiviral agents, most of the focus has been devoted to the repurposing of approved drugs. There are some reports, also,

✉ Mohammad Aghamohammadi
aghamo_m@yahoo.com; tanos@ime.eb.br

1 Department of Chemistry, Borujerd Branch, Islamic Azad University, Borujerd, Iran

2 Independent Researcher, Montreal, QC, Canada

3 Department of Chemistry, Federal Institute of Espirito Santo, Vila Velha, ES, Brazil

4 Graduate Program in Chemistry, Federal University of Espirito Santo, Vitoria, ES, Brazil

5 Université de Québec, INRS – Centre Armand-Frappier Santé Biotechnologie, 531 Boulevard Des Prairies, Laval, Québec H7V 1B7, Canada

6 Laboratory of Molecular Modeling Applied to the Chemical and Biological Defense (LMCBD), Military Institute of Engineering, Rio de Janeiro, RJ, Brazil

7 Department of Chemistry, Faculty of Science, University of Hradec Kralove, Hradec Kralove, Czech Republic

about promising effects of drug combinations, such as hydroxychloroquine and azithromycin [5]. However, the side effects have remained concerning [6]. An alternative way to discover new drugs to combat COVID-19 is to focus on compounds, like vitamins that can be easily found everywhere, are safe to use, do not have high toxicity, and are structurally, as well as, chemically similar enough to the current promising effective antivirals against SARS-COV-2, to mimic their functions.

We have listed some known antivirals, including the ones which have been tried against COVID-19, in Table S1. According to this table, except IFN-alpha (not shown in the table), which is a peptide composed of 165 amino acids, the majority of the antiviral agents are small organic molecules and have at least one alkaloid moiety, including purine, pyrimidine, and imidazole, or one basic amine functional group in their structures. Chloroquine and hydroxychloroquine in particular present another characteristic related to their pKas (which are, respectively, 10.47 and 8.87) for their conjugate acid forms (Table S1). The existence of the basic functional groups in their structures is in agreement with the reported mechanism of their antiviral activity by interfering in the pH-dependent steps of the genome replication [7]. Moreover, having alkaloid moiety and pKa > 8 suggest that at the human body pH, those agents act as bases and exist partially in a protonated form. So, these types of agents might serve as inhibitors of the ACE2 or CD-147 proteins by blocking the negative residues of the proteins' binding sites. However, chloroquine has been reported to have 30-h half-life and recommended to be interrupted at day 5 of treatment of the COVID-19 infection [6] due to the high LogP and LogD and the risk of their accumulation and side effects in the body.

Table S2 list some food supplements which share some structural feature with compounds in Table S1, like the alkaloid function, for example. Among those compounds, three members of the vitamin B family, including vitamin B1 (thiamin), B3 (in the form of nicotinamide), and B6 (preferably in the form of pyridoxamine), exhibit promising properties and have already been reported as having a great potential in the COVID-19 treatment [8–11]. Those molecules have low LogP (−2.1 to 1.3) and LogD (−2.9 to 0.2) compared to that of approved antivirals drugs such as chloroquine (LogP 5.28–3.93), hydroxychloroquine (LogP 3.87–2.89), and even favipiravir (LogP 0.49–0.25). These vitamins present, also, high water solubilities (8.18–500 mg/ml) which are substantially higher than the solubility of chloroquine and hydroxychloroquine (0.0175, 0.0261, respectively), and comparable with favipiravir (8.9 mg/ml) in the case of nicotinamide (8.18 mg/ml). Thiamin's pKa is 4.8, which indicates that it is mainly unprotonated at pH 7.4. However, its intrinsic positive charge on the thiazolium moiety suggests the ability of functioning as ACE2 blocker. This property could make this candidate a very promising option given its huge water solubility and low LogP and LogD. Furthermore, this agent could act as a powerful radical scavenger [12] and limit the harmful oxidative stress-related sequence of receptor-ligand interactions in the infected cells, resulting in apoptosis and/or necrosis, and being followed by the release of the inflammatory and vasodilator agents that is a big issue in COVID-19 infection, and would result in respiratory system failure [13]. Pyridoxamine possesses a basic alkaloid moiety (pKa = 7.02); hence, it will be partially on its protonated form at pH 7.4 and would be considered functioning as an ACE2 blocker. Also, due to its quite high pKa and water solubility as well as low LogP and LogD (−1.1 and −1.4, respectively), pyridoxamine has the potential to intervene in the pH-sensitive steps of the virus genome replication that occurs in the cytoplasm. More importantly, pyridoxamine could mimic favipiravir function as a fake nucleoside to be incorporated in the nascent viral RNA and neutralize it due to possessing nucleophilic NH and OH groups.

Nicotinamide can undergo phosphoribosylation in the target cell by nicotinamide phosphoribosyltransferase [14] to be used as a fake nucleoside. More importantly, nicotinamide has been reported to exert the preventing effect on lung tissue damage in animal models with bleomycin-induced lung injury [15, 16]. The elevated concentration of nicotinamide, as the precursor of $NAD^+$, can lead to the increase of $NAD^+$ levels in the infected cells and activate sirtuins [16]. Finally, the activated sirtuins could be vital for the infected organ to reduce its inflammatory response and finally control inflammation [14]. It has been also reported that nicotinamide can lower the risk of acute kidney injury as one of the life threatening outcomes of COVID-19 infection [10].

Caffeine shows low LogP and LogD (−0.6 in both cases implying the compound is not in its charged form at pH 7.4) and a quite high solubility (58.9 mg/ml), but it does not have either any basic (pKa 0.63 for the most basic nitrogen) or nucleophilic nitrogen. Caffeine has shown radical scavenger activity [17] that is crucial to reduce the oxidative stress in the infected cells [13]. Moreover, caffeine is quickly metabolized in the body by demethylation to produce three metabolites, including paraxanthine (84%), theobromine (12%), and theophylline (4%) [18]. Although these three dimethylxanthine isomers show comparable basicity (pKa = 0.21–0.41 for the most basic nitrogen) to caffeine, indicating that they will be mainly in their neutral form at pH 7.4, paraxanthine and theophylline would have the ability to function as fake nucleobases due to possessing nucleophilic NH groups. However, theobromine, with an iminic NH group, is less likely to be able to undergo a phosphoribosylation reaction.

The first stage of treatment of the disease is the prevention of the virus transmission to the host cells in target organs, especially in the lungs. Therefore, the structure and the type of interactions between ACE2, known as the main gate for the virus entrance, and the spike protein of the virus (*SC2*Spike) have been investigated to give the researchers the sense of which group of compounds could inhibit the interaction and, accordingly, prevent the virus from entering the host cells

[19–21]. Wang et al. compared the interactions of human ACE2 (*Hss*ACE2) with SARS-CoV-2 and SARS-CoV's spike proteins based on crystallography studies [22]. The comparison showed a quite similar pattern of active residues in the spike proteins' RBD interactions with *Hss*ACE2, including 13 hydrogen bonds and 2 salt bridges and 13 hydrogen bonds and 3 salt bridges at the interface of ACE2 with SARS-CoV2 and SARS-CoV, respectively [22–24]. Here, we investigated through molecular docking, molecular dynamics, and free energy MM-PBSA calculations the interactions of caffeine and vitamins B1, B3, and B6 with the residues of the RDB domain of SC2Spike and its complementary binding site in *Hss*ACE2 in order to verify if their binding has potential of interfering in the interactions mentioned above and, consequently, the mechanism of cell invasion of SARS-CoV2.

## Methods

### Docking studies

The compounds under study here were submitted to docking studies on both the RDB binding site of the *SC2*Spike and the binding pocket of the RDB domain in *Hss*ACE-2. The information about the 3D structures of these proteins retrieved from the Protein Data Bank (PDB) [25] for this study are summarized in Table 1. The software used was Molegro Virtual Docker® (MVD), and the protocol was the same validated before [26, 27]. The 3D structures of the ligands were constructed in the Spartan 08 software [28], using the semi-empirical Parametric Method 3 (PM3) [29] for geometry optimization and the Natural Population Analysis (NPA) [30] method for atomic charges calculations. The prevalent species of each compound in physiologic pH, predicted according to the Marvin software (https://chemaxon.com/products/marvin), was used for the docking studies. For caffeine, nicotinamide, and thiamine, the neutral species were prevalent, while for pyridoxamine, both the neutral and the anionic species showed to be present at physiologic pH. The spherical search spaces were centered in the middle of the respective binding sites and involved all the relevant residues of each protein listed in Table 1. For *Hss*ACE-2, the radius of the search space was of 18 Å, while for *SC2*Spyke, it was of 24 Å. Ten runs were performed for each protein–ligand complex on these search spaces, and the 30 best ranked poses were returned for evaluation after each run. These poses were analyzed regarding their MolDock Score and the residues they formed hydrogen bonds (H-bonds) with.

### Molecular dynamic simulations

The 3D structures of the ligands studied were drawn using Avogrado [33] and optimized with GHEMICAL [34] and TRIPOS 5.2 force field [35], followed by semi-empiric optimization with the PM7 method of MOPAC2016 [36]. After, the output files were parameterized to the OPLS-AA force field, using ACPYPE [37] and MKTOP [38].

The complexes protein–ligand were inserted in dodecahedron boxes containing around 15,000 water TIP3P molecules and sodium ions to neutralize the total charge of the system. The energy minimization was performed using the force field OPLS-AA [39] implemented in the GROMACS package [40]. The steps of energy minimization used were: steepest descent (ST) with position-restrained (STPR) and convergence criterion of 600 $kJ.mol^{-1}.nm^{-1}$, ST without PR with the convergence criterion of 300 $kJ.mol^{-1}.nm^{-1}$ and quasi-Newton with a convergence criterion of 41.84 $kJ.\ mol^{-1}.nm^{-1}$. The minimized systems were then submitted to MD simulations in two steps: first 500 ps, at 310 K, with PR of heavy atoms, to allow solvent accommodation around the protein, under periodic boundary conditions, and then 100 ns of full MD simulation at 310 K, with a step integration of 2 fs. The MD simulations were run in triplicate to ensure reproducibility and significance of the results.

As reported before [26, 27], we estimated the binding free energies of each ligand in the respective protein binding pocket after the MD simulations through the MM-PBSA approach [41], which consider the vacuum potential energy, including bonded and non-bonded interactions and free energy of solvation. The g_mmpbsa tool [41] suited for the GROMACS package [40] was used for this task.

**Table 1** Protein structures retrieved from the PDB [31] for this study

| PDB code | Protein | Abbreviation used in this work | Binding pocket | Residues of the binding pocket | Reference |
|---|---|---|---|---|---|
| 6M17 | The 2019-nCoV RBD/ACE2-B0AT1 complex | *Hss*ACE-2 | RDB binding pocket | Gln24, Thr27, Phe28, Asp30, Lys31, His34, Glu35, Glu37, Asp38, Tyr41, Gln42, Leu79, Met82, Tyr83, Asn330, Lys353, Gly354, Asp355, Arg357, Arg393 | [19, 20] |
| 7JZU | SARS-CoV-2 spike in complex with the peptide LCB1 ($IC_{50}$ = 23.5 pM) | *SC2*SPyke | RBD domain | Lys417, Gly446, Tyr449, Tyr453, Leu455, Phe456, Ala475, Phe486, Asn487, Tyr489, Gln493, Gly496, Gln498, Thr500, Asn501, Gly502, Tyr505 | [32] |

**Table 2** Docking results on *Hss*ACE2 and *SC2*Spike

| Comp | *Hss*ACE2 | | | *SC2*Spike | | |
|---|---|---|---|---|---|---|
| | Total energy (kcal/mol) | H-bond energy (kcal/mol) | Interacting residues | Total energy (kcal/mol) | H-bond energy (kcal/mol) | Interacting residues |
| Caffeine | − 79.65 | − 2.08 | Lys353, Arg393 | − 81.62 | − 6.18 | Arg454, Lys458 |
| Nicotinamide Vitamin B3 | − 64.12 | − 7.47 | Asp350, Gly354 Arg393, | − 64.15 | − 8.00 | Arg454, Ile472, Lys458 (2) |
| Pyridoxamine (anion) Vitamin B6 | − 75.16 | − 3.19 | ASp350, Gly354, Asp382, | − 73.78 | − 8.58 | Arg454, Glu471, Ile472, Lys458 (2) |
| Pyridoxamine (neutral) Vitamin B6 | − 89.65 | − 10.56 | Asp350 (3), Asp382, Arg393, Gly354, | − 68.89 | − 6.15 | Arg454, Asp467, Glu471, Lys458 |
| Thiamine (neutral) Vitamin B1 | − 115.65 | − 3.17 | Asp382, Tyr385, Arg393, Gly354 | − 96.47 | − 4.49 | Lys458, Ser469, Arg454 (2), Asp467 |

## Results

### Docking studies

The energy values, interactions, and binding modes obtained for the best poses of the compounds under study after the docking calculations are shown in Table 2 and Figs. 1 and 2. As can be seen, all of them presented negative values of total and H-bond energies in both *Hss*ACE-2 and *SC2*Spyke binding sites. This result suggests that these compounds are capable of binding in both proteins at the respective binding sites of the interface *Hss*ACE-2/*SC2*Spyke. The compound

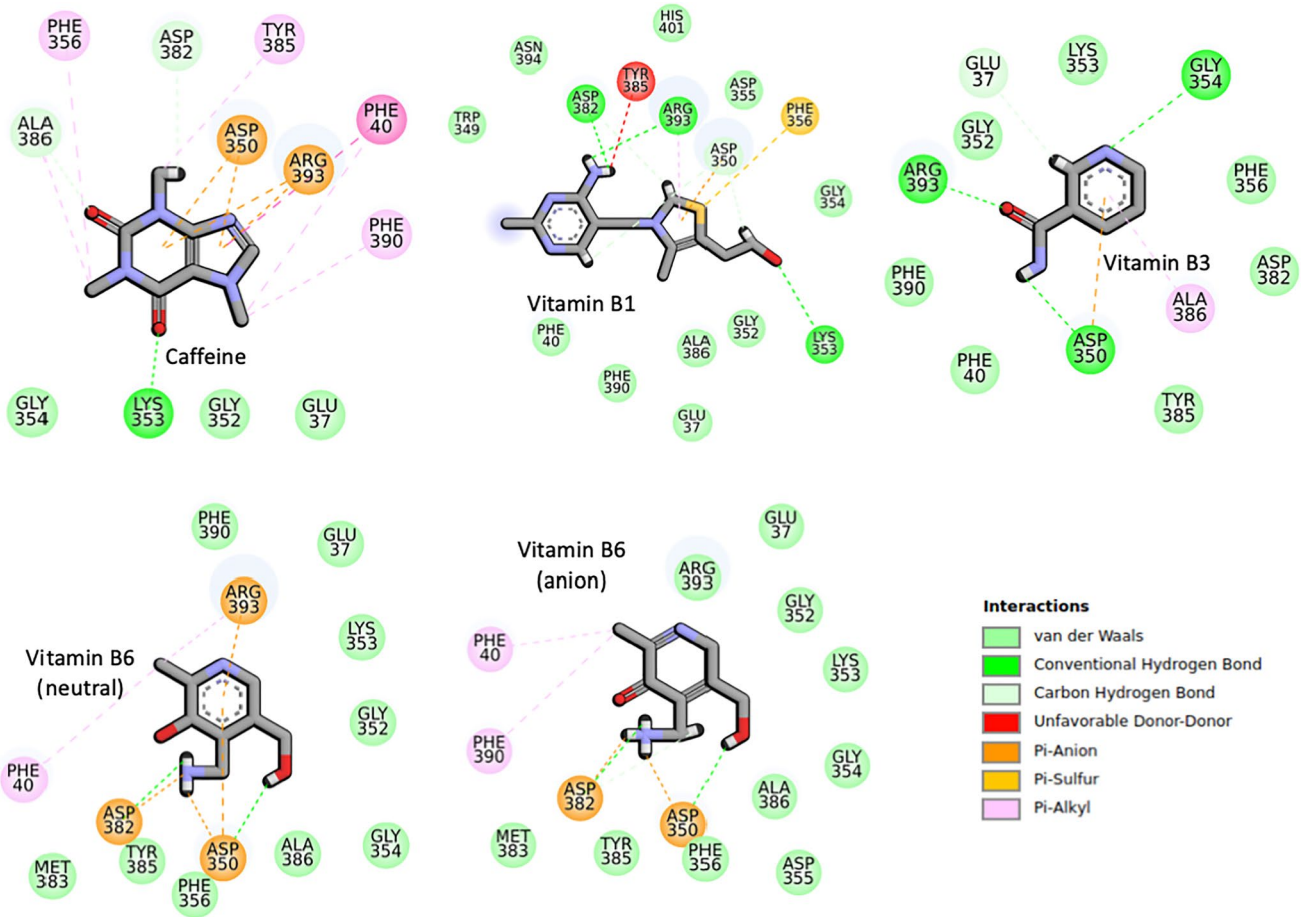


**Fig. 1** Binding maps of the ligands inside *Hss*ACE-2

showing the best result was vitamin B1, with showed total binding energy of − 115 kcal.mol$^{-1}$, inside *Hss*ACE-2 and − 96.47 kcal.mol$^{-1}$ inside *SC2*Spyke. It was followed by vitamin B6 neutral for *Hss*ACE-2 (− 89.65 kcal.mol$^{-1}$) and caffeine for SC2Spyke (− 81.62 kcal.mol$^{-1}$). Results in Table 2 and Figs. 1 and 2 also show that these compounds are capable of stablishing H-bonds with the key residues directly involved in the interactions *Hss*ACE-2/*SC2*Spyke, listed in Table 1, or neighboring residues. This reinforces the hypothesis that these compounds might be capable of disrupting the binding between these two proteins, impairing the invasion of human cells by the SARS-CoV-2.

Interestingly, our results suggest that the best poses of all these nutraceuticals interact with Lys353, and/or Gly354 and/or Arg393, residues that have been proven to be among the characteristic target residues of *Hss*ACE-2 by the *SC2*Spike [19, 20]. This common tendency towards the same residues of *Hss*ACE-2 could provide a strong blocking effect and consequently avoid effective binding of the virus spike proteins to the receptor.

## Molecular dynamic simulations

The MD simulations results showed that none of the ligands was capable of stabilizing in the RDB domain of *SC2*Spike neither keeping interactions with the protein during the simulated time. Regarding *Hss*ACE-2 only vitamins B1 and B6 neutral showed stabilization, while the other ligands also left the protein. Therefore, we are going to discuss here only the MD results obtained for vitamins B1 and B6 neutral.

The energy plots for each system protein/ligand during the MD simulations (data not shown) revealed stabilization at very low energies for both systems since the beginning of the simulations. This is in line with the RMSD plots shown in Figs. 3 and 4, which reflect the good behavior of the ligands in the three MD simulations, with fluctuations never passing 2 Å for vitamin B1 and 1 Å for vitamin B6 neutral. Regarding *Hss*ACE-2, the fluctuations never passed 5.5 and 6.5 Å, respectively.

The plots of H-bonds formed during the MD simulations (Fig. 5) show that both ligands formed a similar number of H-bonds with a slight advantage for vitamin B6 which got closer to keeping 3 H-bonds over most of the simulated time. It also can be observed that this ligand showed a more stable profile of H-bonds compared to vitamin B1. All H-bonds formed during the MD simulations with their respective percentages of occupancy are listed in Table 3. As can be seen, most of the H-bonds pointed in the docking studies were observed. However, vitamin B1 showed a larger diversity

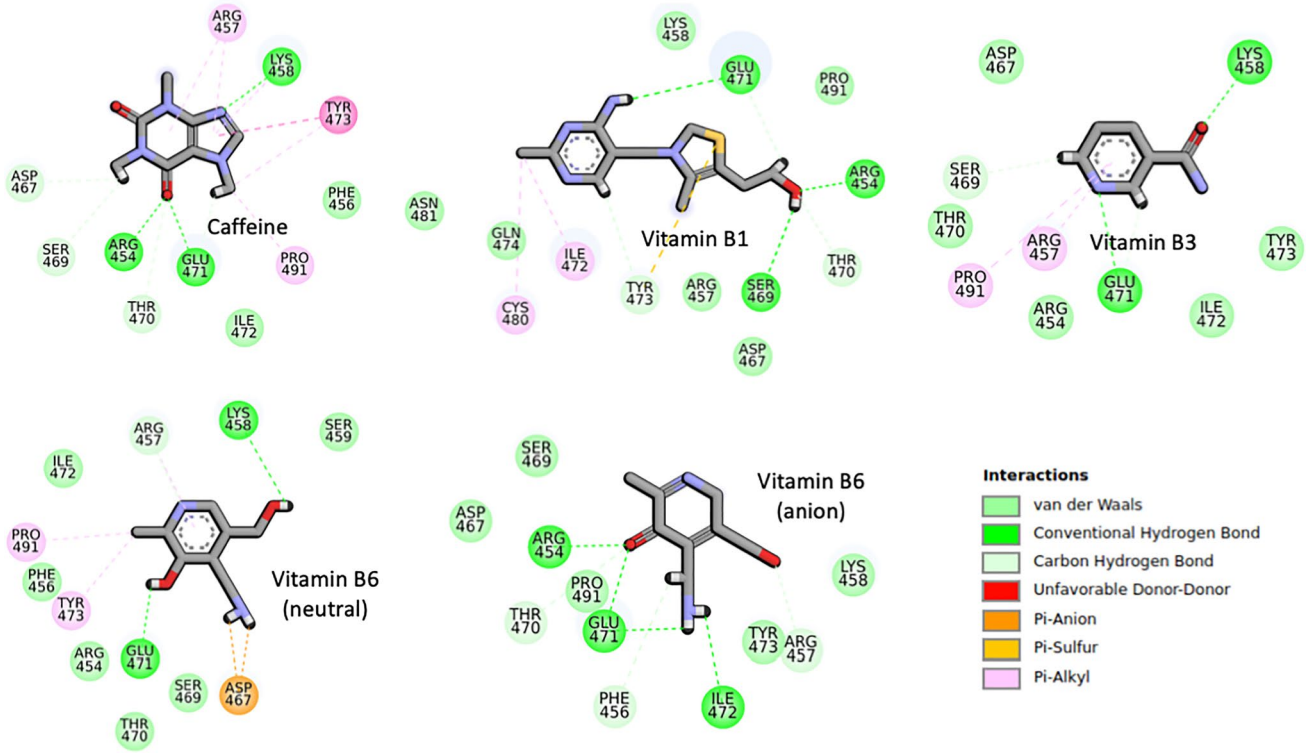


**Fig. 2** Binding maps of the ligands inside *SC2*Spike

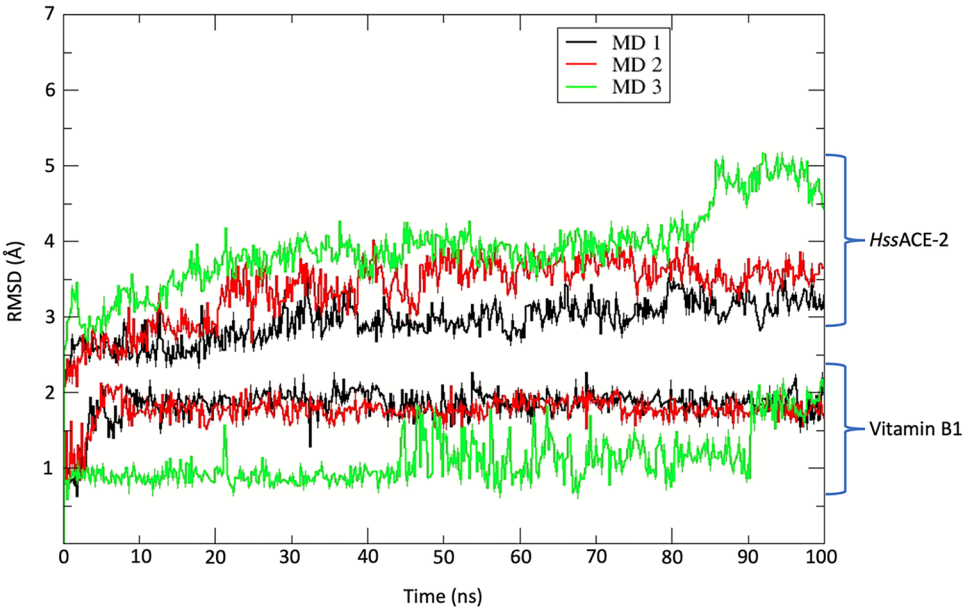


**Fig. 3** RMSD variation for the complex vitamin B1/*Hss*ACE-2 during the three MD simulations

of H-bonding residues, with the most prevalent H-bonds changing from one MD simulation to another. This reflects different behaviors with stabilization in distinct parts of the binding pocket. However, interactions with residues of the binding region of *SC2*Spike, or neighboring residues, were observed in all MD-simulations. Vitamin B6 on the other hand preserved the most prevalent H-bonds with the same group of residues during the simulations (Glu37, Asp350, Asp382) and stabilized in the same region of the pocket which contains most of the residues involved in interactions with the RDB domain of *SC2*Spike.

The contact maps shown in Fig. 6 corroborate the distinct behaviors observed for vitamin B1 in the MD simulations. Those maps show the regions of *Hss*ACE-2 that were up to 4 Å from the ligand during the MD simulations. Analysis of the plots for vitamin B6 neutral shows that in the three MD simulations, this ligand stayed the whole time around the same residues, while vitamin B1 explored other parts of the binding pocket.

Figure 7 show the plots of average total binding energy of each ligand in the binding site of *Hss*ACE-2, calculated through the MMPB-SA methodology [41] from frames

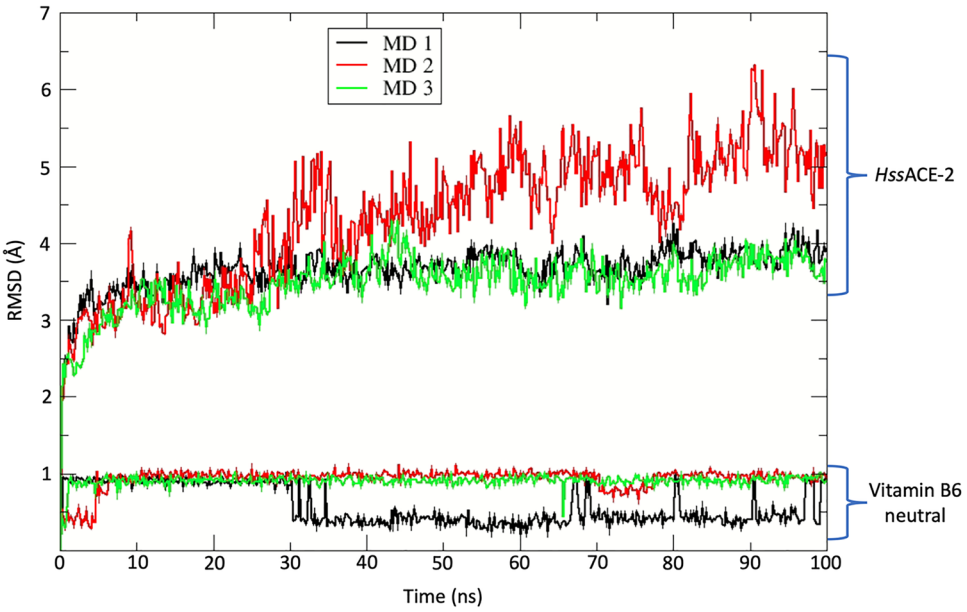


**Fig. 4** RMSD variation for the complex vitamin B6 neutral/*Hss*ACE-2 during the three MD simulations

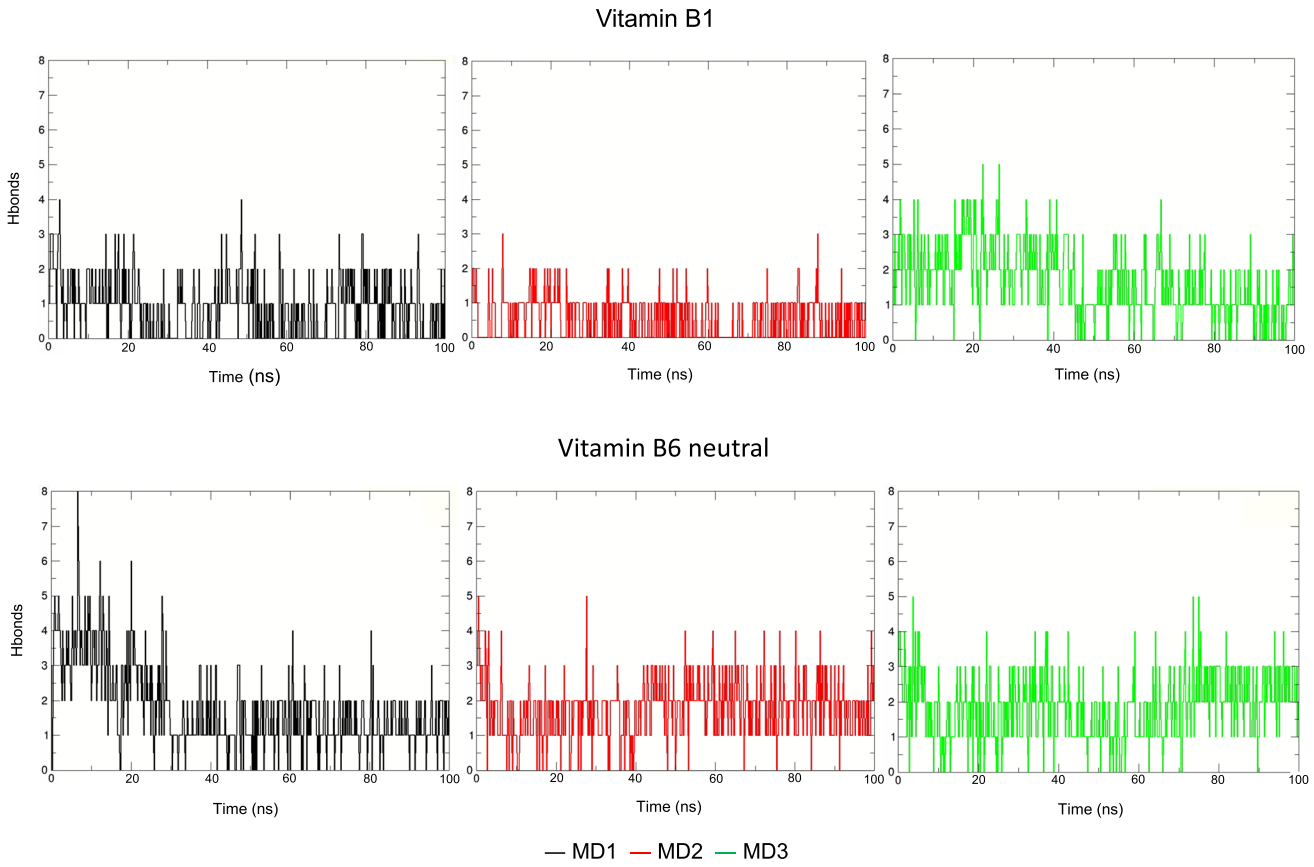


**Fig. 5** Plots of number of H-bonds formed by each ligand during the 100 ns of MD simulation in the binding site of *Hss*ACE-2

collected during the MD simulations. The negative values observed are qualitatively aligned with the docking results for these ligands confirming their affinities for the binding site of *Hss*ACE-2. It is also observable that the values for vitamin B6 neutral converged to around − 145 kcal.mol$^{-1}$ in the three MD simulations, while no convergence was observed for

**Table 3** H-bonds formed during the MD simulations. Percentage values > 100% indicate that more than one H-bond was formed with the residue

| Comp | Interacting residues | | |
|---|---|---|---|
| | MD1 | MD2 | MD3 |
| Vitamin B1 | Ala99(1.20%), Asn103(9.08), Ala348(2.20%), Trp349(0.20%); Asp350(40.72%), Asp382(14.97%), Tyr385(0.40%), Phe390(4.59%), Leu391(0.80%), Arg393(6.59%); Asn394(10.18%) | Gln98(0.40%), Ala99(0.20%), Gln102(3.00%), Asn103(1.40%), Tyr196(4.79%), Tyr202(21.36%), Asp206(1.40%), Asp350(1.20%), Arg393(0.60%), Asn394(1.20%), Glu398(16.77%), His401(0.20%), Arg514(0.40%) | Phe40(0.60%), Ala99(2.99%), Gln102(0.60%), Asn103(8.18%), Asp206(1.00%), His345(0.20%), Ala348(19.96%), Asp350(61.67%), Lys353(0.20%), Phe356(0.20%), Asp382(55.69%), Tyr385(0.20%), Ala386(0.20%), Phe390(1.20%), Leu391(0.20%), Arg393(7.78%), Asn394(1.00%), Glu398(0.20%), Asp509(2.59%) |
| Vitamin B6 | Glu37(9.78%), Tyr41(0.80%), Ser44(0.80%), Ala348(1.20%), Trp349(0.60%), Asp350(50.50%), Lys353(0.40%), Asp382(106.19%), Arg393(7.58%), His401(0.20%) | Glu37(21.56%), Phe40(0.20%), Tyr41(0.40%), Asp350(56.69%), Lys353(0.80%), Asp382(95.01%), Arg393(2.79%), | Glu37(48.70%), Phe40(0.20%), Asp350(71.06%), Lys353(0.20%), Asp382(55.49%), Tyr385(0.40%), Ala386(0.20%), Arg393(9.58%) |

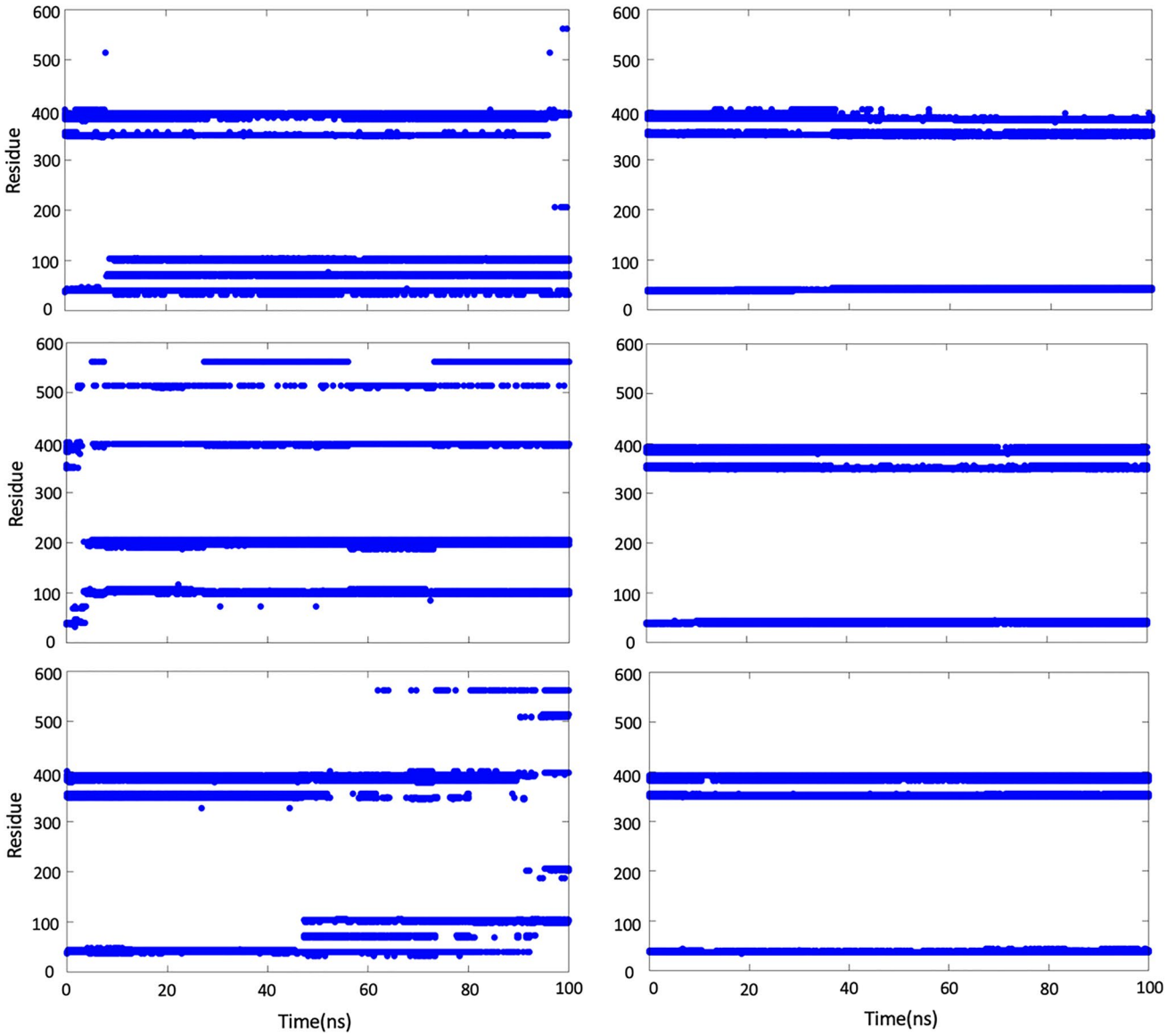


**Fig. 6** Contact maps for the systems protein–ligand during the MD simulations. Left, vitamin B1; right, vitamin B6 neutral

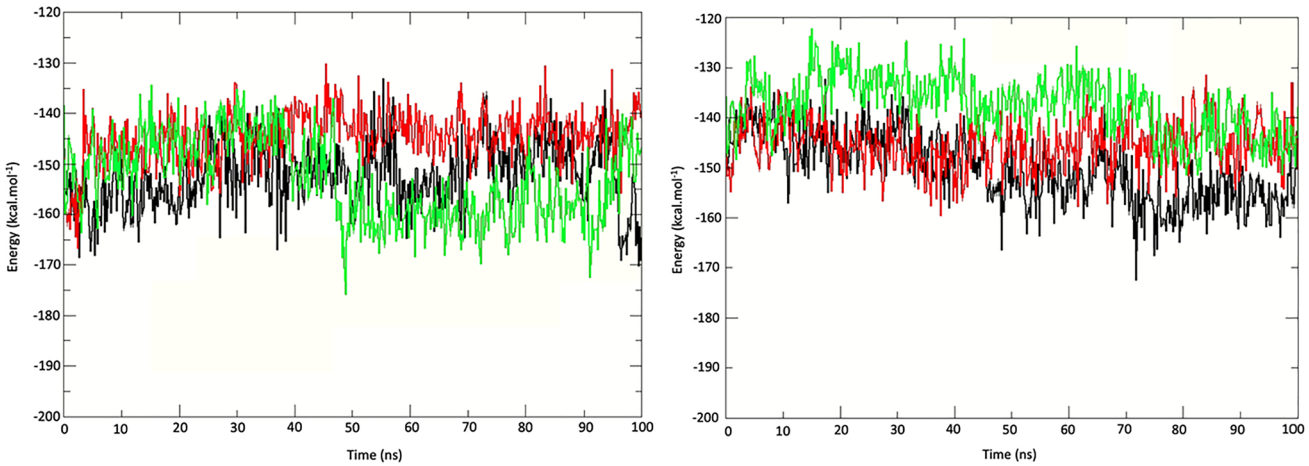


**Fig. 7** Plots of average total energy calculated by the MM-PBSA approach for vitamin B1 (left) and vitamin B6 neutral (right) inside *Hss*ACE-2

vitamin B1. This reflects the fact that in each MD simulation, this ligand stabilized in a different region of the *Hss*ACE-2 binding site.

## Conclusions

Our results suggest that vitamins B1 and B6 in the neutral form are capable of binding to key residues of *Hss*ACE-2 in the region responsible for interactions with the RDB domain of *SC2*Spike that leads to the cellular invasion of human cells by the SARS-CoV-2. The docking studies showed that all the nutraceuticals initially investigated have negative interacting energies in the RDB domain of *SC2*Spike and its corresponding binding site in *Hss*ACE-2, showing interactions with key residues in both sites. However, the MD simulations showed that none is capable of stabilizing in the RDB domain of *SC2*Spike and that only vitamins B1 and B6 in the neutral form are capable of stabilizing in the binding site of *Hss*ACE-2. This was further corroborated by the free energy values obtained through the MM-PBSA approach [41]. We believe that our results not only are in line with some reports in the literature pointing this type of molecule as potential treatments for COVID-19 [8–11], but also highlight them as excellent leads for the drug design of new and more potent inhibitors of the mechanism of cellular invasion of SARS-CoV-2.

**Supplementary Information** The online version contains supplementary material available at https://doi.org/10.1007/s00894-022-05356-9.

**Acknowledgements** The authors wish to thank the Islamic Azad University of Borujerd, the Brazilian agencies, FAPERJ, grant number E-02/202.961/2017, FAPES-BPC-Pq, grand number 06/2021, IFES-PRPPG, grant number 12/2020 - Researcher Productivity Program, PPP, and FAPES, grant number 03/2020-2020-WMT5F, for infrastructure and financial support, and Professor Salwa Karboune from McGill University for the time and valuable comments. This work was also supported by the University of Hradec Králové. We also thank the University Federal of Lavras (UFLA)—Brazil for software facilities.

**Author contribution** All authors contributed to the study conception and design. Material preparation, data collection, and analysis were performed by Mohammad Aghamohammadi, Mehdi Sirouspour, Arlan S. Goncalves, and Tanos C. C. Franca. The first draft of the manuscript was written by Mohammad Aghamohammadi, Mehdi Sirouspour, and Tanos C. C. Franca and revised by Steven R. LaPlante. All authors commented on previous versions of the manuscript. All authors read and approved the final manuscript.

**Funding** This work was supported by the Islamic Azad University of Borujerd, and the Fundação de Amparo a Pesquisa do Estado do Rio de Janeiro (FAPERJ), grant number E-02/202.961/2017.

**Data availability** The datasets generated during and/or analyzed during the current study are available from the corresponding author on reasonable request.

## Declarations

**Competing interests** The authors declare no competing interests.

## References

1. Guo L et al (2021) Engineered trimeric ACE2 binds viral spike protein and locks it in "three-up" conformation to potently inhibit SARS-CoV-2 infection. Cell Res 31(1):98–100
2. Gordon DE et al (2020) A SARS-CoV-2 protein interaction map reveals targets for drug repurposing. Nature 583:459–468
3. Chen YW, Bennu YC, Wong KY (2020) Prediction of the SARS-CoV-2 (2019-nCoV) 3C-like protease (3CL pro) structure: virtual screening reveals velpatasvir, ledipasvir, and other drug repurposing candidates. 9:129
4. Elfiky AA (2020) Anti-HCV, nucleotide inhibitors, repurposing against COVID-19. Life Sci 248:117477
5. Gautret P et al (2020) Hydroxychloroquine and azithromycin as a treatment of COVID-19: results of an open-label non-randomized clinical trial. Int J Antimic Agents 56:105949
6. Andrea Cortegiani GI (2020) Mariachiara Ippolito, Antonino Giarratano, Sharon Einav, A systematic review on the efficacy and safety of chloroquine for the treatment of COVID-19. J Crit Care 57:279–283
7. Savarino A et al (2003) Effects of chloroquine on viral infections: an old drug against today's diseases. Lancet Infect Dis 3(11):722–727
8. Shakoor H et al (2021) Be well: A potential role for vitamin B in COVID-19. Maturitas 144:108–111
9. Bogan-Brown K et al (2022) Potential efficacy of nutrient supplements for treatment or prevention of COVID-19. J Dietary Supp 19(3):336–365
10. Raines NH et al (2021) Niacinamide may be associated with improved outcomes in COVID-19-related acute kidney injury: an observational study. Kidney360,2(1):33–41
11. Miller R, Wentzel AR, Richards GA (2020) COVID-19: NAD+ deficiency may predispose the aged, obese and type2 diabetics to mortality through its effect on SIRT1 activity. Med Hypotheses 144:110044
12. Okai Y et al (2007) Potent radical-scavenging activities of thiamin and thiamin diphosphate. J Clin Biochem Nutrition 40(1):42–48
13. Kouhpayeh SS L, Boshtam M, Rahimmanesh I, Mirian M, Zeinalian M, Salari-jazi A, Khanahmad N, Damavandi MS, Sadeghi P, Khanahmad H (2020) The molecular story of COVID-19; NAD+ depletion addresses all questions in this infection. Preprints 2020:2020030346
14. Gallí M et al (2010) The nicotinamide phosphoribosyltransferase: a molecular link between metabolism, inflammation, and cancer. Can Res 70(1):8–11
15. Nagai A et al (1994) Effects of nicotinamide and niacin on bleomycin-induced acute injury and subsequent fibrosis in hamster lungs. Exp Lung Res 20(4):263–281
16. Shi Y et al (2020) COVID-19 infection: the perspectives on immune responses. Cell Death Differ 27(5):1451–1454
17. Liu R et al (2019) Binding characteristics and superimposed antioxidant properties of caffeine combined with superoxide dismutase. ACS Omega 4(17):17417–17424
18. White JR et al (2016) Pharmacokinetic analysis and comparison of caffeine administered rapidly or slowly in coffee chilled or hot versus chilled energy drink in healthy young adults. Clin Toxicol 54(4):308–312

19. Yan R et al (2020) Structural basis for the recognition of SARS-CoV-2 by full-length human ACE2. Science 367(6485):1444–1448
20. Lan J et al (2020) Structure of the SARS-CoV-2 spike receptor-binding domain bound to the ACE2 receptor. Nature 581(7807):215–220
21. Han Y, Král P (2020) Computational design of ACE2-based peptide inhibitors of SARS-CoV-2. ACS Nano 14(4):5143–5147
22. Wang K et al. (2020) CD147-spike protein is a novel route for SARS-CoV-2infection to host cells. Signal Transduct Target Ther 5:283
23. Wang Q et al (2020) Structural and functional basis of SARS-CoV-2 entry by using human ACE2. Cell 181(4):894-904.e9
24. Davidson AM, Wysocki J, Batlle D (2020) Interaction of SARS-CoV-2 and other coronavirus with ACE (angiotensin-converting enzyme)-2 as their main receptor. Hypertension 76(5):1339–1349
25. Berman HM et al (2000) The Protein Data Bank. Nucleic Acids Res 28(1):235–242
26. Botelho FD et al (2020) Ligand-based virtual screening, molecular docking, molecular dynamics, and MM-PBSA calculations towards the identification of potential novel ricin inhibitors. Toxins 12(12):746
27. Almeida JSFD et al (2022) Searching for potential drugs against SARS-CoV-2 through virtual screening on several molecular targets. J Biomol Struct Dyn 40(11):5229–5242
28. PC Spartan pro Molecular Modeling for the Desktop (1999) Chem Engineering News Archive 77(17):2
29. Stewart JJP (2004) Optimization of parameters for semiempirical methods IV: extension of MNDO, AM1, and PM3 to more main group elements. J Mol Model 10:155–164
30. Reed AE, Weinstock RB, Weinhold F (1985) Natural population analysis. J Chem Phys 83(2):735–746
31. Berman HM et al (2002) The protein data bank. Acta Cryst D58, 899–907
32. Cao B et al (2020) A trial of lopinavir–ritonavir in adults hospitalized with severe COVID-19. N Engl J Med 382(19):1787–1799
33. Hanwell MD et al (2012) Avogadro: an advanced semantic chemical editor, visualization, and analysis platform. J Chemin 4(1):17
34. Hassinen T, Peräkylä M (2001) New energy terms for reduced protein models implemented in an off-lattice force field. J Comput Chem 22(12):1229–1242
35. Shih JH, Chen CL (1995) Molecular dynamics simulation of bisphenol A polycarbonate. Macromolecules 28(13):4509–4515
36. Stewart JJP (2013) Optimization of parameters for semiempirical methods VI: more modifications to the NDDO approximations and re-optimization of parameters. J Mol Model 19(1):1–32
37. Sousa Da Silva AW and WF Vranken (2012) ACPYPE - AnteChamber PYthon Parser interfacE. BMC Res Notes 5:367
38. Ribeiro AAST, Horta B AC, RB De Alencastro (2008) MKTOP: a program for automatic construction of molecular topologies. J Brazilian Chem Soc 19(7):1433–1435
39. Robertson MJ, Tirado-Rives J, Jorgensen WL (2015) Improved peptide and protein torsional energetics with the OPLS-AA force field. J Chem Theory Comput 11(7):3499–3509
40. Abraham MJ T Murtola and R Schulz (2015) GROMACS: high performance molecular simulations through multi-level parallelism from laptops to supercomputers. SoftwareX 1-2:19–25
41. Kumari R, Kumar R, Lynn A (2014) g_mmpbsa—a GROMACS tool for high-throughput MM-PBSA calculations. J Chem Inf Model 54:1951–1962